

On the effect of neglecting anharmonic nuclear motion in charge density studies

Kathrin Meindl, Regine Herbst-Irmer and Julian Henn*

Georg-August Universität Göttingen, Tammannstrasse 4, 37077 Göttingen, Germany. Correspondence e-mail: jhenn@chemie.uni-goettingen.de

The effect of neglecting anharmonic nuclear motion when it is definitely present is studied. To ensure the presence of anharmonic nuclear motion a model was used that was previously refined against experimental data including anharmonic nuclear motion, and these calculated structure factors were used as observed data for a multipole refinement. It was then studied how the neglect of anharmonic nuclear motion and noise in the data affects the usual crystallographic quality measure R , the density parameters and the residual density distribution. It is demonstrated that the neglect of anharmonic nuclear motion leads to a characteristic imprint onto the residual density distribution in terms of residual density peaks and holes, in terms of the whole residual density distribution and in terms of the number, location and strength of valence shell charge concentrations (VSCCs). These VSCCs differ from that of the input model in a way which heavily influences and misleads the chemical interpretation of the charge density. This imprint vanishes after taking anharmonic nuclear motion into account. Also the input model VSCCs are restored. The importance of modeling anharmonic nuclear motion is furthermore shown by the characteristic imprint on the residual density distribution, even in the case of a numerically almost unaffected R value.

© 2010 International Union of Crystallography
Printed in Singapore – all rights reserved

1. Introduction

In some of our recent charge density studies we experienced difficulties in appropriately refining the model to a flat and featureless residual density. In 9-diphenylthiophosphinoyl-anthracene unreasonably high residual density peaks remained close to the sulfur atoms (Herbst-Irmer *et al.*, 2009). The topological analysis of an aluminumphosphanide, **1** (Henn *et al.*, 2010), showed in addition to the peak and hole at the P atom an unexpected number of valence shell charge concentrations (VSCCs), which was also not in accordance with the theoretical results. Both problems could be solved by introducing anharmonic nuclear motion *via* the Gram–Charlier expansion (Johnson & Levy, 1974).

The refinement of anharmonic nuclear motion in charge density studies has already been discussed in the literature (Kuhs, 1988, 1992; Sørensen *et al.*, 2003; Whitten *et al.*, 2006; the list is by no means complete), sometimes with contradicting results. Mallinson *et al.* (1988) claim that anharmonic nuclear motion can be modeled by density parameters and therefore should not be simultaneously refined with them, at least not in the presence of strong parameter correlations. Restori & Schwarzenbach (1996) state that anharmonic nuclear motion, libration and disorder cannot be distinguished from each other by a single X-ray experiment, as all of these

might cause a deviation of the atomic probability density function (p.d.f.) from a Gaussian shape. The p.d.f. is the Fourier transform of the Debye–Waller factor, *i.e.* its real-space representation. In contrast to their findings, Iversen *et al.* (1999) were able to separate anharmonic nuclear motion effects from electron-deformation effects with the use of only a single-temperature X-ray data set; however, they deal with very high resolution (1.7 \AA^{-1}), very heavy atoms (Th) and very low experimental temperatures (9 and 27 K). We experienced that this separation is also possible with much lower resolution (1.15 \AA^{-1}), lighter atoms (P) and a higher experimental temperature (100 K) (Henn *et al.*, 2010). Bürgi *et al.* (2000) even decompose anisotropic displacement parameters into contributions from low-frequency high-amplitude vibrations and their anharmonicity from high-frequency low-amplitude motion as well as from inadequately modeled absorption and extinction using multi-temperature data.

In our study we allow for a general position of the atom moving anharmonically. We are investigating the effects of neglecting present anharmonic nuclear motion on the refined parameters, the residual density distribution and the topology of the aforementioned aluminumphosphanide ($\text{PAlN}_2\text{C}_{12}\text{H}_{14}$). Also correlations between density parameters and thermal motion parameters are monitored and discussed in detail.

2. Method

2.1. Density parameters and topological analysis

Whereas density parameters are dependent on the parametrization, a topological analysis, which gives maxima, minima and saddle points, is not. It is possible to discuss topological results without even mentioning the parametrization of the density. Therefore, a topological analysis of the electron density is a compact parameter-free description of the rather complicated distribution and can serve as a basis for a comparison of electron densities, for example from theory and experiment or from different density models. As understood in this sense, a topological analysis is an interpretation-free method to explore and characterize a density distribution. In this context we discriminate between density distributions differing quantitatively and qualitatively. For example, when the values of the electron density at a saddle point differ for two models, but in general there are equal numbers of those saddle points, maxima and minima, the difference is regarded to be only quantitative. Quantitative differences in the topology are expected for different models. If, however, the number of topological objects is different for two models, this case corresponds to a structural difference. Major occurrences of this type exist when the number of maxima or saddle points in the density differs. When a different number of maxima, minima or saddle points in higher derivatives of the electron density, like in the Laplacian, appears, we regard this as minor occurrences. The models, although possibly quite similar in their parametrization, are then qualitatively different. This latter case happens, for example, when the topology of two density models is of the same type but the topology of the Laplacian, *i.e.* the number of VSCCs, differs.

2.2. Procedure

To investigate the effects of neglecting anharmonic nuclear motion although it is present, we employed theoretical data from a compound containing phosphorus and aluminium. The 'theoretical data' were obtained from the final multipole model of the metallaphosphane $\text{Me}_2\text{Al}(\mu\text{-py})\text{P}$ (space group $P2_1/c$, measured at 100 K with Mo $K\alpha$ up to a resolution of 1.15 \AA^{-1}). The experimentally determined $\sigma(I)$ were also used for the 'theoretical' reflection file. For more experimental and crystallographic details see Henn *et al.* (2010). We start from a reference model that includes a Gram–Charlier expansion to fourth order at the phosphorus atom and to third order at the aluminium atom. This model fitted best our experimental data. Calculated structure factors for this model were used in subsequent refinements as observed structure factors (data set 1). In a second data set, Gaussian noise in proportion to the square root of the intensity is added to the respective intensity (data set 2). The procedure of adding noise is described in detail by Meindl & Henn (2008); the process is controlled and characterized by the noise-control parameter p_1 , which was chosen to be 0.333 throughout. The noise leads to a small number of negative-intensity observations, which are excluded from the refinement. The noise was chosen such that it resembles the noise found in the experiment. The parameters

for the reference model, *i.e.* the density (coordinates, monopoles and multipoles) and thermal motion parameters (U_{ij} , C_{ijk} , D_{ijkl}), are taken from the experiment.

The refinements were performed using *XD2006* (Volkov *et al.*, 2006) against F^2 with $I/\sigma(I) > 0$ up to the experimental resolution of $\sin \theta/\lambda = 1.15 \text{ \AA}^{-1}$, starting from the correct reference model and adjusting coordinates, harmonic motion parameters, anharmonic nuclear motion parameters (in those cases where these have been refined) to respective order, κ for all atoms, multipoles up to hexadecapoles for P, Al, N and methyl C atoms, and up to octupoles for the remaining phenyl C atoms applying a local mirror plane in the phenyl rings, and bond-directed dipoles for H atoms. Nine κ sets for non-H atoms were refined. For the H atoms κ values were taken from the literature (Volkov *et al.*, 2001). The values for κ' were taken from the experimental results and kept fixed. The coordinates of the H atoms were reset to neutron distances to the corresponding C atoms, and harmonic motion parameters were set according to $U_{\text{iso}}(\text{H}) = 1.5U_{\text{eq}}(\text{C}_{\text{methyl}})$ and $1.2U_{\text{eq}}(\text{C}_{\text{phenyl}})$. For the refinements the density and thermal motion parameters as well as the R -factor ($R = [\Sigma(|F_{\text{obs}}| - |F_{\text{calc}}|)]/\Sigma|F_{\text{obs}}|$) were monitored. Furthermore, a residual density analysis (Meindl & Henn, 2008) was carried out for different models to characterize the effects of neglecting anharmonic nuclear motion and/or noise.

In the following, the density and thermal motion parameters are shown and discussed for the different refinements in the form of tables and pictures. The models employed are briefly described:

(i) Refinement **a** is the reference model. The model includes anharmonic nuclear motion to fourth order for the P atom and to third order for the Al atom. This model was refined against data set 1, which excludes noise.

(ii) Refinement **b** uses a model completely neglecting anharmonic nuclear motion. The density and thermal motion parameters are adjusted by a least-squares refinement against data set 1. This refinement serves to show the pure effect of neglecting anharmonic thermal motion in terms of density values, thermal motion values, the R value and the residual density analysis descriptors $d^f(\rho_0)$, $\Delta\rho_0$ and e_{gross} (Meindl & Henn, 2008).

(iii) Refinement **c** uses the same model as **a** but the refinement, like refinements **d**, **e** and **f**, was performed against data set 2, *i.e.* Gaussian noise is added to the ideal intensities and a refinement of all density and thermal motion parameters including full anharmonic nuclear motion is performed.

(iv) Refinement **d** corresponds to data set 2 (*i.e.* noisy data). In this model only anharmonic nuclear motion at the Al atom is neglected, whereas anharmonic nuclear motion to fourth order at the P atom is retained.

(v) In refinement **e**, in addition to the neglect of anharmonic nuclear motion at the Al atom, fourth-order Gram–Charlier parameters are also neglected for the P atom while the third order is still present.

(vi) Finally, refinement **f** completely excludes anharmonic nuclear motion. In contrast to **b**, however, data set 2 is used. The difference between this model and model **c** is that model **c**

Table 1

 Crystallographic R values for the reference model and refinements **b–f**.

 R is given in %. GC: Gram–Charlier parameters.

	a	b	c	d	e	f
Noise ($p_1 = 0.333$)	Off	Off	On	On	On	On
Third-order GC	P/Al	Off	P/Al	P	P	Off
Fourth-order GC	P	Off	P	P	Off	Off
R	0.00	0.35	1.54	1.54	1.55	1.56

contains all anharmonic thermal motion whereas this model excludes anharmonic nuclear motion completely.

The situation corresponding to model **a** is highly idealized and serves as a reference, whereas the situation described in **c** is the optimum one could reach in the laboratory. Model **f** corresponds to the realistic situation in which anharmonic nuclear motion has not been considered although it is present. It is the situation an experimenter might be confronted with during a charge density study.

3. Results

3.1. Effect on the crystallographic R value

Table 1 shows the crystallographic R values for all refinements and the reference model.¹ The noise was chosen such that it leads to an R factor similar to the experimental one. In the absence of noise the neglect of anharmonic motion leads to a significant increase in the R factor of 0.35% (**b**). In the presence of noise, however, the differences are marginal. A model completely neglecting anharmonic motion (**f**) leads to an R value of 1.56%, whereas the complete model including anharmonic motion to fourth order at the P atom and to third order at the Al atom results in $R = 1.54\%$ (**c**), with a total difference of only 0.02%.

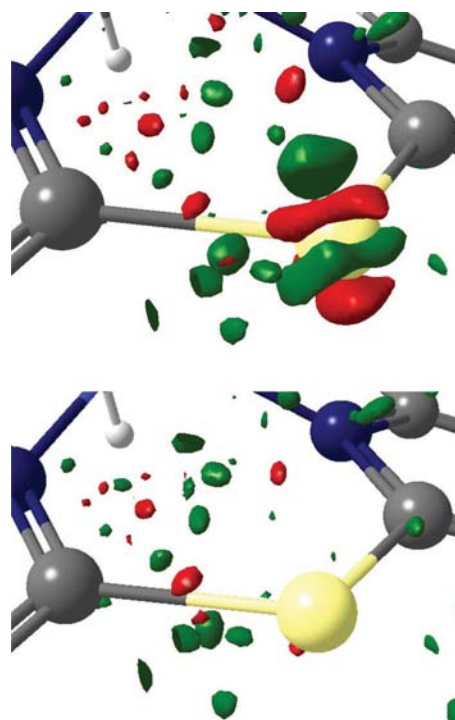
3.2. Effect on the residual density distribution and the topology

Fig. 1 shows a residual density isosurface in the vicinity of the P atom. The alternating occurrence of positive (green) and negative (red) residual density (shashlik pattern) seems to be typical for unmodeled anharmonic nuclear motion (Herbst-Irmer *et al.*, 2009) of third order. This corresponds to refinement **f**, the situation one may be confronted with in a charge density study when anharmonic nuclear motion is not considered, although present. This pattern was also observed, although not published, in the experiment leading to the publication of Henn *et al.* (2010). The residual density shashlik pattern disappears after inclusion of anharmonic nuclear motion Gram–Charlier parameters (refinement **c** and Fig. 1, bottom).

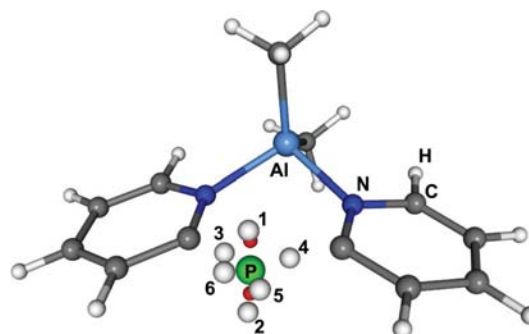
Fig. 2 shows the locations of the VSCCs (white spheres) together with the positions of the largest peak and deepest

hole (red spheres) when anharmonic nuclear motion is neglected. The peak distances to the P atom and strengths are: 0.50 Å and 0.23 e Å⁻³ (above molecular plane), and 0.39 Å and -0.21 e Å⁻³ (below plane). When noise is excluded (refinement **b**) the values are 0.51 Å and 0.24 e Å⁻³, and 0.42 Å and -0.27 e Å⁻³. Table 2 shows the influence of anharmonic nuclear motion on the residual density and the number, strength and location of VSCCs close to the P atom for all refinements.

In refinement **a** there are four VSCCs around the P atom, which is in accordance with gas-phase optimizations (Henn *et al.*, 2010). Their positions are depicted in Table 2. For all


Figure 1

Isosurface representation of the residual density. Top: shashlik pattern around the P atom, which is located in a nodal plane between the red and green surfaces at the center; green: 0.088 e Å⁻³, red: -0.106 e Å⁻³; the representation corresponds to refinement **f**. Bottom: the same isosurfaces after refinement **c**. The figure was created using *Mollso* (Hübschle & Luger, 2006).


Figure 2

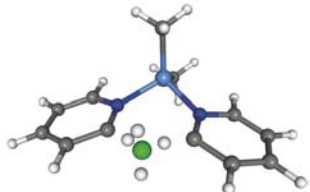
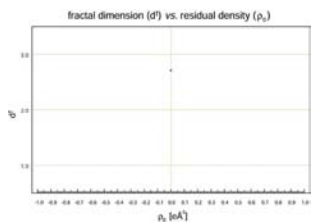
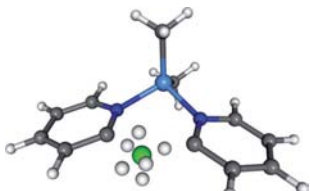
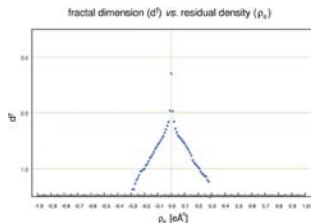
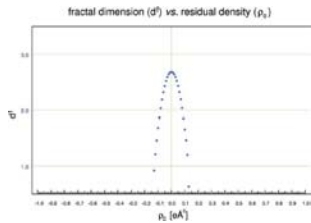
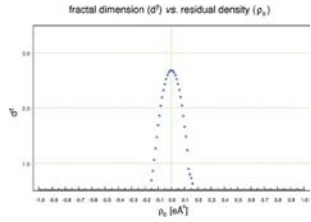
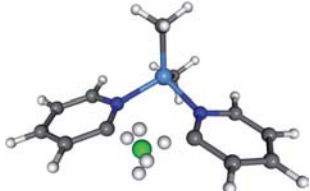
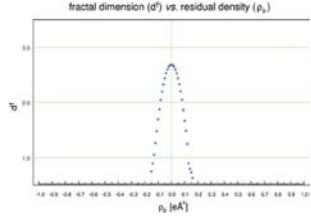
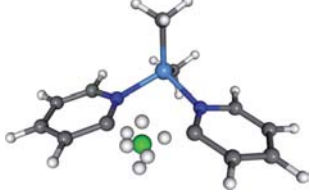
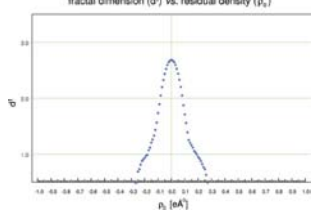
The positions of the largest peak and hole (red spheres) together with the VSCCs (white spheres around green P atom) in the phosphanide, after refinement of model **f**.

¹ Table 1 in the supplementary material shows the numerical values of selected geometry, density and thermal motion parameters of the P atom for the different refinements together with the estimated standard uncertainties. Histograms for higher multipoles are also shown (Reference: SH5102). Services for accessing these data are described at the back of the journal.

Table 2

 The number, location and strengths of the VSCCs and residual density analysis plots for the whole unit cell corresponding to refinements **a–f**.

 Only the VSCCs related to the P atom are shown as white spheres. The numbering in column three is according to the scheme of Fig. 2. The Laplacian $\nabla^2\rho$ is given at the VSCCs and the eigenvalues $\lambda_1, \lambda_2, \lambda_3$ of the second derivative of the Laplacian with respect to the coordinates.

Refinement	$\nabla^2\rho$ ($e \text{ \AA}^{-5}$); $\lambda_1, \lambda_2, \lambda_3$ ($e \text{ \AA}^{-7}$)	$d^f(\rho_0)$ versus ρ_0
a 	1: -5.1; 23.7, 50.7, 634.9 2: -5.6; 28.8, 57.0, 667.1 3: -5.3; 68.1, 122.8, 485.3 4: -7.2; 71.7, 141.4, 636.1	
b 	1: -5.4; 36.0, 58.8, 661.8 2: -5.2; 31.1, 60.3, 646.1 3: -4.5; 64.4, 113.9, 416.4 4: -6.3; 62.4, 134.2, 559.9 5: -3.5; 18.2, 37.9, 533.7 6: -3.7; 13.6, 43.4, 546.7	
c Same as a	1: -5.2; 14.4, 60.7, 646.6 2: -5.7; 28.9, 64.0, 677.6 3: -6.6; 90.5, 139.9, 637.7 4: -6.8; 57.7, 141.6, 626.1	
d Same as a	1: -5.2; 14.4, 60.2, 645.6 2: -5.7; 28.4, 63.8, 676.5 3: -6.6; 90.5, 140.5, 637.8 4: -6.9; 57.5, 142.0, 626.8	
e 	1: -5.2; 16.7, 61.2, 650.1 2: -6.0; 30.1, 69.0, 698.2 3: -6.4; 93.0, 136.8, 613.0 4: -6.9; 55.5, 142.5, 624.5 5: -3.0; 8.1, 33.5, 503.0	
f 	1: -5.2; 19.2, 62.2, 648.1 2: -5.1; 23.5, 61.0, 640.9 3: -5.7; 81.6, 128.5, 543.8 4: -5.9; 46.6, 132.6, 538.8 5: -3.2; 12.2, 38.2, 512.3 6: -4.0; 2.0, 32.3, 569.1	

refinements not properly describing anharmonic nuclear motion at the P atom, different numbers of VSCCs (varying between 5 and 6) are found, none of which correspond to the correct number of four VSCCs. In Table 2 the values for $\nabla^2\rho(\mathbf{r}_{\text{VSCC}})$ are given additionally, together with the eigenvalues of $\nabla^4\rho(\mathbf{r}_{\text{VSCC}})$. For the calculation of the extrema of a

function, it is necessary to calculate the second derivatives of this function to show the extremal nature at the point in question; for the Laplacian being the function discussed, this obviously implies the calculation of the fourth derivatives of the density with respect to the coordinates. These eigenvalues of the fourth derivatives are given. Their units are $e \text{ \AA}^{-7}$. They

must not be confused with the eigenvalues of the Laplacian with units $e \text{ \AA}^{-5}$. Their sum can be taken as a measure of the distinctness of the extremum in the same sense as for the Laplacian and its eigenvalues. A particularly low eigenvalue may indicate that the extremum is actually close to being a saddle point. The extremal nature of such a point with a low eigenvalue may be questionable if approximations enter the procedure. In the last column of Table 2 a residual density analysis plot of the whole unit cell is shown (Meindl & Henn, 2008). As model **a** is the reference model without noise in the data, only a single point is characterizing the residual density corresponding to an entirely flat and featureless residual density distribution. The improper description of the anharmonic nuclear motion can also be seen in the fractal dimension plots. Only refinement **c**, which includes anharmonic nuclear motion to third order for the Al and P atoms and to fourth order for the P atom, results in a Gaussian distribution of residuals, as indicated by the parabolic shape in the residual density plot.

Refinement **f**, which neglects anharmonicity completely but includes experimental noise and multipole expansion to the hexadecapole level, shows six VSCCs around the P atom in a distorted octahedral geometry, with one apex above and one below the molecular plane spanned by the P atom and its adjacent C atoms. One VSCC is located in each of the respective P–C bonds, which leaves four non-bonding VSCCs. Two of these are located approximately in directions extending the bond directions; the remaining two are at the apexes. The values range between -3 and $-6 e \text{ \AA}^{-5}$; the two smallest values have particularly small eigenvalues λ_1 and λ_2 whereas in λ_3 all six VSCCs are of the same order of magnitude. Note that for the calculation of these values the fourth derivatives of the electron density with respect to the coordinates have to be calculated numerically, which is prone to errors. The $d^f(\rho_0)$ versus ρ_0 plot shows distinct shoulders in the periphery. Refinement **f**, where anharmonic nuclear motion is excluded, shows the same features that we had noticed in our experimental investigation of 9-diphenylthiophosphinoylanthracene and aluminumphosphanide: shoulders in the residual density distribution and an unusual number of VSCCs. This distribution should be compared with refinement **b**, which gives the values for noise-free data. The shoulders are largely reduced when third-order Gram–Charlier coefficients are refined for the P atom (**e**). Only a small deviation from a parabolic shape remains in the positive residual density regime. Simultaneously, one of the VSCCs lying in the C–P bond extension disappears.

If additionally fourth-order Gram–Charlier coefficients are refined for the P atom (**d**), the other VSCC lying in the bond extension also vanishes. The smallest eigenvalue is now $14.4 e \text{ \AA}^{-7}$, whereas before it was 8.1 (**e**) and $2.0 e \text{ \AA}^{-7}$ (**f**). The tiny shoulder in the positive residual density regime, however, remains.

Additional refinement of third-order anharmonic nuclear motion parameters for the Al atom restores a parabolic shape in the residual density distribution without shoulders (**c**). The values of the VSCCs should be compared with the true values

obtained without noise (**a**). The comparison shows how the small noise in the data corresponding to an R value of approximately 1.5% influences the Laplacian.

Fig. 3 shows schematically the Gaussian p.d.f., modified separately by the influence of anharmonic nuclear motion (top: third order; bottom: fourth order). The blue distribution must be convoluted with the static density distribution to obtain the final peak and hole. It can be seen from the curve, however, that the peak and hole will be approximately at the same distance in opposite directions of the atom from neglect of third-order terms. In contrast, residual density peaks from fourth-order terms at opposite directions have the same sign. Note that residual density peaks on opposite sides and with opposite signs are exactly what one would expect for the case of neglecting third-order anharmonic nuclear motion (see Fig. 3, top). Therefore, the appearance of such peaks and holes should be taken as a characteristic sign for the possible neglect of anharmonic nuclear motion. The location of the maximum of the p.d.f. is shifted by third-order Gram–Charlier contributions (Fig. 3, top). This establishes a correlation between third-order Gram–Charlier coefficients and coordinates. Similarly, a correlation between fourth-order Gram–Charlier coefficients and U_{ij} exists. This can be seen from Fig. 3 (bottom).

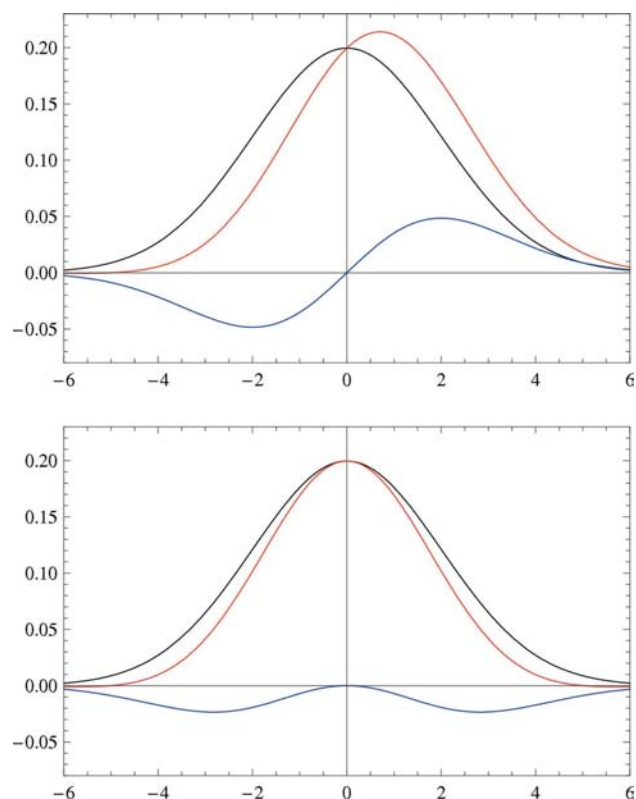


Figure 3

Gaussian probability density function (p.d.f.) (black), deviation from Gaussian p.d.f. (blue), and resulting total p.d.f. (red) corresponding to a third-order (top) and fourth-order (bottom) anharmonic nuclear motion. The parameters chosen are as follows. Gaussian p.d.f.: $f(x) = \sigma^{-1}(2\pi)^{-1/2} \exp -x^2/2\sigma^2$; third-order curve: $0.2 x f(x)$; fourth-order curve: $-0.04 x^2 f(x)$.

In refinement **f**, the peak (distance 0.51 Å, strength $\sim 0.24 \text{ e \AA}^{-3}$) and the hole (distance 0.42 Å, strength $\sim -0.27 \text{ e \AA}^{-3}$) on opposite sides of the phosphorus atom and to a very good approximation lying on a straight line through the atomic center *remained* regardless of the density parameters as long as anharmonic nuclear motion was *not* taken into account. This is a counter-example of the opinion that the multipole model is in general flexible enough to describe anharmonic nuclear motion artificially by density parameters.

3.3. Effects on thermal motion parameters

3.3.1. Anisotropic thermal motion parameters, U_{ij} . Fig. 4 shows the six individual components for P with standard deviations given as error bars. As the errors are very small, the error bars have been magnified 100-fold. The yellow columns (reference model **a**) show the true values, therefore no error bars are given. The neglect of anharmonic nuclear motion (dark green, refinement **b**) introduces an error and slightly reduces the total harmonic thermal motion as given by $U_{\text{eq}} = 1/3(U_{11}^{\text{C}} + U_{22}^{\text{C}} + U_{33}^{\text{C}})$ (where C indicates Cartesian coordinates; for the values in crystal coordinates see Table 1 of the supplementary material). This small reduction is maintained for all refinements regardless of whether these include or exclude anharmonicity. However, all following refinements include noise and the small reduction may be attributed as well to the presence of noise. That noise may dominate the model behavior will be seen again in §3.3.2. Introducing noise while refining the correct model (red, refinement **c**) increases the standard deviation but has no further effect. Switching off anharmonic nuclear motion at the Al atom (blue, refinement **d**) has no distinct effect on the thermal anisotropic displacement parameters or their standard deviations at the P atom. Switching off the fourth-order Gram–Charlier expansion at the P atom while refining third-order parameters at the P atom

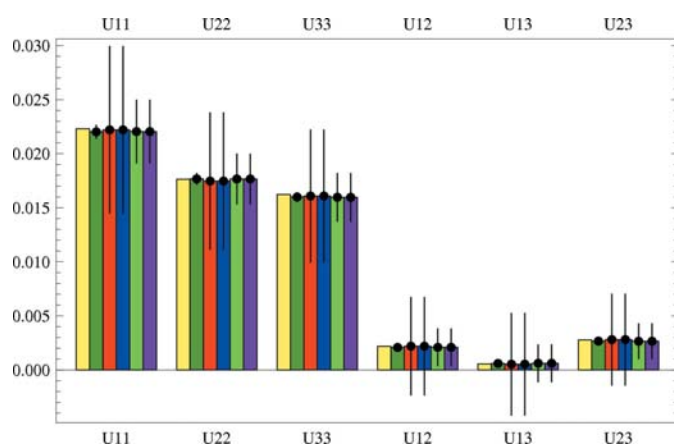


Figure 4
Thermal anisotropic displacement parameters U_{ij} at the P atom from the reference model (refinement **a**, yellow), from refinements excluding noise in the data (refinement **b**, dark green), and including noise and different levels of anharmonic nuclear motion at the P and at the Al atom [refinements **c** (red), **d** (blue), **e** (light green) and **f** (purple)]. The error bars have been magnified by a factor of 100.

(light green, refinement **e**), however, reduces the error bars roughly by a factor of 0.5. There are two possible reasons for the decrease in uncertainty: a reduced number of model parameters (15 parameters fewer to determine) and reduction of parameter correlation. As already stated it is found that fourth-order Gram–Charlier coefficients correlate with the harmonic motion parameters, which are of second order, as both represent powers of 2 in the coordinates. The reduction in the standard uncertainties seems to be due to these correlations, as there is no further reduction in the error bars when the third order is also excluded (purple, refinement **f**) despite reducing the model by a further 20 parameters.

In total, a slightly reduced harmonic thermal motion as expressed by U_{eq} results for all refinements **b–f**.

3.3.2. Third-order Gram–Charlier coefficients, C_{ijk} . The ten components of the third-order Gram–Charlier expansion at the P atom are given in the order C_{111} , C_{222} , C_{333} , C_{112} , C_{122} , C_{113} , C_{133} , C_{223} , C_{233} , C_{123} . The yellow column in each block of Fig. 5 shows the original reference value. The red bar shows the value after refinement of the full model against noisy data, the following bar (blue) shows the values after a refinement (against noisy data) where anharmonic nuclear motion at the Al atom has been neglected, and, finally, the last (light green) bar shows the effect of the neglect of fourth-order anharmonic nuclear motion at the P atom again against noisy data. The inclusion of (experimental) noise (red) has a distinct effect on the values, which sometimes even differ in their sign from the true value (see C_{222} and C_{122}). The standard deviation that is in contrast to the U_{ij} given without a magnifying factor varies over a wide range: in particular C_{111} and C_{222} have large standard deviations, while those for the remaining parameters are much smaller. Despite the small absolute values, five out of ten parameters are significantly larger than their respective standard uncertainty if a 3σ criterion is applied. These are C_{112} , C_{113} , C_{133} , C_{233} , C_{123} . It is remarkable that the details of the model seem to be of less importance than the introduction of noise as is indicated by the similar behavior of all models, in particular where this is in contrast to the true values as for the components C_{222} and C_{122} . When the value of one model is

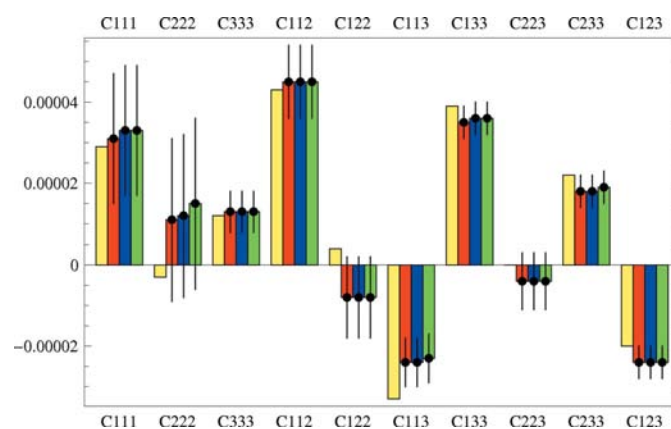


Figure 5
Gram–Charlier coefficients C_{ijk} for refinements **a** (yellow), **c** (red), **d** (blue) and **e** (light green).

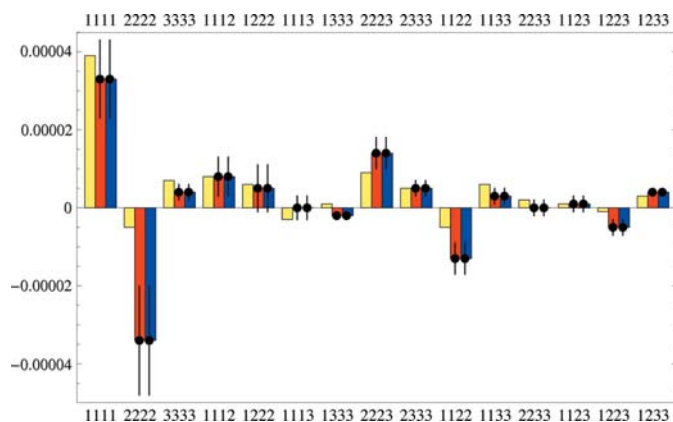


Figure 6 Fourth-order Gram–Charlier coefficients for refinements **a** (yellow), **c** (red) and **d** (blue).

larger than the true value, then all models yield larger values and similarly for the smaller values.

3.3.3. Fourth-order Gram–Charlier coefficients, D_{ijkl} . The third-order anharmonic nuclear motion parameters have already been found to be small; however, not surprisingly, most of the fourth-order parameters are even smaller. The reader might doubt whether these small values may possibly have any impact on the density or residual density at all. Only because this is indeed the case is the description of these parameters included. Fig. 6 shows a comparison of the coefficients D_{ijkl} between true values (yellow) and values obtained from a refinement against noisy data with (red) and without anharmonic nuclear motion of the Al atom (blue) given in the order: $D_{1111}, D_{2222}, D_{3333}, D_{1112}, D_{1222}, D_{1113}, D_{1333}, D_{2223}, D_{2333}, D_{1122}, D_{1133}, D_{2233}, D_{1123}, D_{1233}, D_{1233}$. The introduction of noise (red column) has a particular strong effect on component D_{2222} . Also D_{2223} and D_{1122} seem to be affected. The exclusion of anharmonic nuclear motion at the Al atom (blue) has no effect on the fourth-order Gram–Charlier parameters of the P atom. Only four parameters are significant according to a 3σ criterion. These are $D_{1111}, D_{2223}, D_{1122}, D_{1233}$. If a 1σ criterion was applied, all but the four weakest contributions ($D_{1222}, D_{1113}, D_{2233}, D_{1123}$) are significant.

In summary, it must be stated that all the parameter values for the true anharmonic nuclear motion of the phosphorus atom are very small.

3.4. Density parameters

To allow for a comparison of the numerous density parameters, we use a distance measure between two sets of density parameters similar to the R value. For this, the absolute differences of the parameter values from the true values are added for all multipoles except for the monopole (for an explanation see further down), *i.e.* we added the absolute residuals. The statistical significance of the parameter values is not considered in this procedure. However, an easy-to-interpret dimensionless single number is assigned to each set of multipoles (24 parameters). This number should be as small

Table 3

Quality measures and parameter residuals of the different refinements.

R is given in %, $\Delta\rho_0 = \rho_{0,\max} - \rho_{0,\min}$ in \AA^{-3} , and $e_{\text{gross}} = \frac{1}{2} \int_{V_{\text{UC}}} |\rho_0(\mathbf{r})| \, d\mathbf{r}$ in e. The integration is over the whole unit cell. ρ_0 : residual density; $\rho_{0,\max}$: largest peak; $\rho_{0,\min}$: deepest hole. The R values for the multipole parameters are dimensionless. For a definition of these and for more information see text. GC: Gram–Charlier parameters.

	a	b	c	d	e	f
Noise ($p_1 = 0.333$)	Off	Off	On	On	On	On
Third-order GC	P/A1	Off	P/A1	P	P	Off
Fourth-order GC	P	Off	P	P	Off	Off
$d'(0)$	2.71	2.70	2.68	2.68	2.68	2.68
$\Delta\rho_0$	0.00	0.58	0.27	0.32	0.32	0.54
e_{gross}	0.25	1.69	15.83	15.87	15.91	16.00
R_{dip}	0	0.043	0.032	0.032	0.035	0.070
R_{quad}	0	0.047	0.027	0.026	0.060	0.061
R_{octu}	0	0.129	0.067	0.067	0.068	0.099
R_{hexa}	0	0.043	0.122	0.121	0.111	0.106
R_{sum}	0	0.262	0.194	0.195	0.249	0.302

as possible in order for the set to be as close to the original values as possible. For density values identical to the true values, this measure yields zero. The R values were calculated for the different multipoles P_{lm} . R_{dip} denotes the R value of the three dipoles P_{1m} , R_{quad} is the R value for the five quadrupoles P_{2m} , R_{octu} is the R value for the seven octupoles P_{3m} , and R_{hexa} the R value for the nine hexadecapoles P_{4m} . For each multipole P_{lm} the R_{lm} value was calculated according to the formula $R_{lm} = \sum_{m=-l}^{+l} |P_{lm}(\text{reference}) - P_{lm}(\text{actual})|$. The sum is obtained according to $R_{\text{sum}} = \sum_{l=1}^4 R_{lm}$.

The changes in the monopole are of a different order of magnitude than the rather small changes in the higher multipoles, which describe a shift of density rather than an amount of density, and therefore have to be treated separately. The absolute residual sum is given in Table 3 (last row). The neglect of anharmonic nuclear motion gives a residual sum of 0.262 (refinement **b**). This value is taken as reference. Noise in the data and the inclusion of anharmonic nuclear motion allow for a shift in the parameter values which results in the lower $R_{\text{sum}} = 0.194$ (**c**), *i.e.* the overall similarity of the multipole model parameters to the true values has increased. Neglecting third-order anharmonic nuclear motion at the Al atom slightly increases the absolute residual sum to 0.195 (**d**). There is, however, a jump in the absolute residual sum to 0.249 (**e**) when fourth-order anharmonic nuclear motion at the phosphorus atom is neglected and an even higher jump to $R_{\text{sum}} = 0.302$ (**f**) if additionally the third order is also omitted. These results show that inclusion of anharmonic nuclear motion at the P atom is important for obtaining density parameters as close as possible to the true values, even though the true anharmonic nuclear motion parameters are very small. Compare also with Table 2 for the effect on the topology.

The residual sum can further be decomposed into the contributions from the multipoles (see Table 3). For example, the total residual sum of refinement **b**, which gives the pure effect of neglect of anharmonic nuclear motion, is decomposed into the contributions $R_{\text{dip}} = 0.043$, $R_{\text{quad}} = 0.047$, $R_{\text{octu}} = 0.129$ and $R_{\text{hexa}} = 0.043$. The octupole parameters change as much as all other parameters together. From the octupoles, in

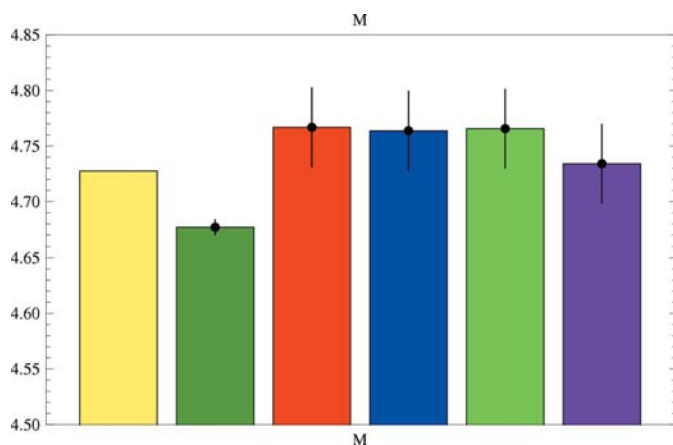


Figure 7
Monopole populations for refinements **a** (yellow), **b** (dark green), **c** (red), **d** (blue), **e** (light green) and **f** (purple). Error compensation leads to the best monopole value for the worst model (**f**).

turn, $O1+$ and $O1-$ contribute over 50% to the total of $R_{\text{octu}} = 0.129$. However, after inclusion of experimental noise, the most pronounced changes in the parameters are in the hexadecapoles (**c**, **d**, **e**) until anharmonic nuclear motion is again completely neglected and residuals in the octupoles contribute as much as from hexadecapoles (**f**).

3.4.1. Monopoles, M . The monopole is a more fundamental parameter than the other density parameters, as all higher multipoles rely on the population of the monopole. The total neglect of anharmonic nuclear motion and exclusion of noise in the data results in a decreased monopole (**b**, dark green in Fig. 7) in comparison with the true value (**a**, yellow) and in a very small standard uncertainty. Inclusion of noise increases the monopole to higher than the true value (**c**, red, **d**, blue, **e**, light green). The standard deviations are obviously determined by the noise. The under- and overestimation of the monopole seem to compensate when anharmonic nuclear motion is completely neglected in the presence of noise (**f**, purple).

3.4.2. Dipoles. The dipole component $D0$ of the true model is close to zero (see Fig. 8). Comparison of the dark green (**b**) and the purple (**f**) bars shows that noise in the data affects the dipole $D1+$ and $D1-$ only moderately; however, $D0$ is affected most. The orientation of $D0$ is close to the direction in which the largest residual density holes and peaks also occur, above and below the molecular plane spanned by the P and the N atoms (see Fig. 2). It is therefore reasonable to assume that the density model tries to compensate for the neglect of anharmonic nuclear motion by shifting density from the largest peak to the deepest hole, which are both located close to the phosphorus atom and almost in opposite directions. This can be seen in Fig. 8 from a comparison of the noise-free refinement **b** neglecting anharmonic nuclear motion (dark green) and all refinements containing noise and at least third-order parameters at the P atom (**c**, red, **d**, blue, **e**, light green), which are all closer to the true value (**a**, yellow) for $D0$. For this dipole $D0$, the fourth-order anharmonic nuclear motion at the P atom is also obviously very important, as can be seen

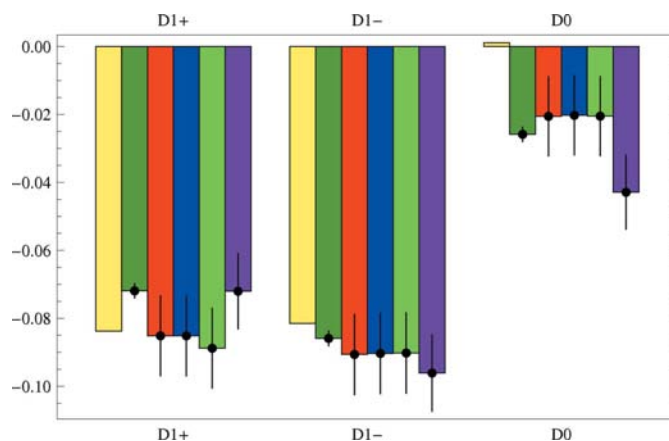


Figure 8
Dipole populations for refinements **a–f**. If anharmonic nuclear motion is neglected completely in the presence of noise, the dipole $D0$ tries to compensate for the model shortcomings (see purple bar).

from the jump of the purple bar (refinement **f**) to a value differing most from the true value (**a**, yellow). The flexibility of the multipole model is not sufficient for a complete compensation of neglect of anharmonic nuclear motion and residual density peaks remain until anharmonic nuclear motion at least to third order at the P atom is included (see Table 2). Note that in this case the inflexibility of the multipole model is an advantage, as it indicates model errors.

3.4.3. Quadrupoles, octupoles and hexadecapoles. Histograms and additional information for these density parameters are given in the supplementary material. The higher multipoles are increasingly dominated by the noise. It is difficult to extract general tendencies from these data as the changes owing to a neglect of anharmonic motion scatter over the whole parameter set, whose values are additionally dependent on the orientation of the local coordinate systems. All these subtle changes together lead to the appearance of artificial VSCCs around the P atom. No distinct correlations between multipole parameters and anharmonic nuclear motion parameters were observed.

4. Correlation

Strong correlation between model parameters may lead to insignificant results. In the literature such strong correlations of 90% and more among thermal motion parameters (U_{11}/D_{1111} 0.90) and a high correlation between a density parameter and harmonic motion parameters (P_{20} correlated with U_{22} and U_{23} of the Fe atom with coefficients -0.90 and -0.93) are reported (Mallinson *et al.*, 1988). According to Mallinson *et al.*, these high correlations prevented convergence in a first attempt to refine multipole parameters and anharmonic nuclear motion parameters simultaneously. They solved this problem by initially refining anharmonic nuclear motion parameters against high-order data only and, in a subsequent step, to allow for a simultaneous refinement of all parameters.

In the case of high parameter correlation one has to be very careful about the conclusions drawn from such a refinement.

In our studies, however, no such strong correlations were observed. The largest coefficients found are between 0.85 and 0.82 for U_{ii} and D_{iii} , $i = 1, 2, 3$, followed by a correlation coefficient between 0.76 and 0.70 for coordinates and C_{iii} (x with C_{111} , y with C_{222} , z with C_{333}) both being in the same range as monopole and κ correlations. Next is the rather small correlation between U_{ij}/D_{iii} and U_{ij}/D_{ijj} in the range 0.68 to 0.65. Generally, we find correlations among coordinates and third-order Gram–Charlier coefficients as well as between harmonic motion parameters and fourth-order Gram–Charlier coefficients, in accordance with their representation of even and odd powers of x , y and z . The correlation between C_{ijk} and x , y , z has already been illustrated in Fig. 3. This figure also illustrates the potential correlation between D_{ijkl} and U_{ij} and between D_{ijkl} and κ or κ' . Since there are no distinct correlations between anharmonic nuclear motion and density parameters, and since no convergence problems were experienced, these were refined simultaneously. After 20 cycles of refinement of all parameters together excluding κ' , the maximum shift per standard uncertainty was only 10^{-10} . That this procedure is feasible in the present case in spite of the experience described in the literature was ultimately confirmed from the refinements, as the residual density peaks and holes close to the P atom (see Fig. 2) were not absorbed into the density model.

5. Conclusion

Anharmonicity and multipole parameters may sometimes be able to describe the same features; however, if the features are in reality caused by anharmonicity, the anharmonic refinement will be superior, even at the given experimental conditions, which correspond to 100 K data and a resolution of 1.15 \AA^{-1} , as demonstrated in the present paper. As the R values are only slightly affected by the anharmonic nuclear motion, the superiority of one refinement over the other cannot be established by the R factors. A residual density analysis is able to reveal the different distributions of the residual densities from the different refinements. Naturally, the refinement is to be preferred which has a Gaussian distribution of residuals, appearing as a parabola in the residual density analysis plots. What causes the differences in the residual density distribution and how reliable are they? The valence density is mainly described by relatively few low-order data. The anharmonic nuclear motion, in contrast, is described by a convolution of the whole static (pseudo-)atomic density including the core density with the probability density function describing the total motion. This affects mainly high-order data. These are often known to a lower statistical significance which, however, is counterbalanced by the relative abundance of high-order data. Thus, if a very large number of high-order reflections are under- or overestimated by the model, this is of statistical significance even if every individual deviation is not significant. Therefore, provided anharmonic nuclear motion is present, this is better described by a refinement including anharmonic nuclear motion than by a model that erroneously tries to take anharmonic nuclear motion into account by

density parameters. The reasons are (i) even though density parameters may reduce the absolute height of residual density peaks and holes generated by the neglect of anharmonic nuclear motion, the resulting residual density distribution is non-Gaussian and (ii) even if the residual density distributions were not too far from a Gaussian, the models affect different ranges in reciprocal space (low-order *versus* high-order data) and therefore tend to separate naturally in the present case. It can be assumed that both reasons are more important for data with less noise and with higher resolution. The low noise in the data may be the most important single reason for the strong impact of anharmonic nuclear motion parameters in the present case. Exceptions may occur, for example when the residual density maxima generated by the neglect of anharmonic nuclear motion are at a distance which fits very well to the maximum of a radial function. But even in this case the residuals will be distributed differently.

The neglect of present anharmonic nuclear motion results in a distinct residual density distribution with characteristic imprint. Neglect of third-order Gram–Charlier coefficients results in a peak and a hole at opposite sides of the atom in question. In the present case the distances of these to the nucleus were typically $0.4\text{--}0.5 \text{ \AA}$ and of about the same strength, although a tendency can be observed to lower absolute values for the holes. An isosurface representation of the residual density typically shows a shashlik-like structure of alternating positive and negative residual density values with the atomic position in a nodal plane (see Fig. 1). The plot of the fractal dimension *versus* the residual density shows very characteristic shoulders of a triangular shape superimposed by the noise (see Table 2, which shows the pure effect of neglecting anharmonic nuclear motion, refinement **b**, the pure effect of noise, **c**, and the combined effect of neglecting anharmonic nuclear motion in the presence of noise, **f**).

If these parameters describing anharmonic nuclear motion are not included, the refinement yields the wrong number of VSCCs around the P atom. For a complete neglect of anharmonic nuclear motion four non-bonding VSCCs are obtained, for a neglect of fourth-order parameters three non-bonding VSCCs are obtained, and, finally, only in the case of full anharmonic refinement to fourth order is the correct number of two non-bonding VSCCs obtained. It is expected that this type of error would be even more distinct for heavier atoms.

The large correlations between density and anharmonic nuclear motion parameters reported in the literature were not observed in this case.

The present case is characterized by a very low noise level in the data, leading to an R factor of approximately 1.5% and by small anharmonic nuclear motion coefficients. It is a question for future research whether or not the conclusions drawn from this also hold in cases where the resolution of the data set or its quality are lower. As pointed out in §2.1, a topological analysis may serve as a parameter-free analysis method. To our knowledge the influence of anharmonic motion modeling on the density model has been discussed in the literature so far mainly with respect to (multipole) model parameters. We suggest employing a topological analysis in future. The most

important conclusions drawn from this study are: density and anharmonic nuclear motion parameters separate naturally in reciprocal space, at least in the present case; even for atoms as heavy as phosphorus anharmonic nuclear motion affects the residual density significantly at the given resolution. Both conclusions lead to the important statement that it is indeed possible to separate bonding and anharmonic nuclear motion effects in a single diffraction experiment. Finally, as the inclusion of anharmonicity affects the crystallographic *R* values only slightly, it is more appropriate to analyze the residual density distribution, which clearly reveals neglect of anharmonic nuclear motion in charge density studies.

We acknowledge support from the DFG Schwerpunktprogramm SPP 1178. We thank Professor Stalke for the encouragement to work on this topic. The authors thank Professor Sheldrick for discussions and support. We thank the referees and the editor for many helpful suggestions.

References

- Bürgi, H. B., Capelli, S. C. & Birkedal, H. (2000). *Acta Cryst.* **A56**, 425–435.
- Henn, J., Meindl, K., Schwab, G., Oechsner, A. & Stalke, D. (2010). *Angew. Chem. Int. Ed.* **49**, 2422–2426.
- Herbst-Imer, R., Henn, J., Kratzert, D., Stern, D. & Stalke, D. (2009). 2009 ACA Meeting, July 2009, Toronto, Ontario, Canada, Talk w0141.
- Hübschle, C. B. & Luger, P. (2006). *J. Appl. Cryst.* **39**, 901–904.
- Iversen, B. B., Larsen, F. K., Pinkerton, A. A., Martin, A., Darovsky, A. & Reynolds, P. A. (1999). *Acta Cryst.* **B55**, 363–374.
- Johnson, C. K. & Levy, H. A. (1974). *Thermal Motion Analysis Using Bragg Diffraction Data*. In *International Tables for X-ray Crystallography*, Vol. IV, pp. 311–336. Birmingham: Kynoch Press.
- Kuhs, W. F. (1988). *Aust. J. Phys.* **41**, 369–382.
- Kuhs, W. F. (1992). *Acta Cryst.* **A48**, 80–98.
- Mallinson, P. R., Koritsanszky, T., Elkaim, E., Li, N. & Coppens, P. (1988). *Acta Cryst.* **A44**, 336–343.
- Meindl, K. & Henn, J. (2008). *Acta Cryst.* **A64**, 404–418.
- Restori, R. & Schwarzenbach, D. (1996). *Acta Cryst.* **A52**, 369–378.
- Sørensen, H. O., Stewart, R. F., McIntyre, G. J. & Larsen, S. (2003). *Acta Cryst.* **A59**, 540–550.
- Volkov, A., Abramov, Y. A. & Coppens, P. (2001). *Acta Cryst.* **A57**, 272–282.
- Volkov, A., Macchi, P., Farrugia, L. J., Gatti, C., Mallinson, P. R., Richter, T. & Koritsanszky, T. (2006). *XD2006. A Computer Program Package for Multipole Refinement, Topological Analysis of Charge Densities and Evaluation of Intermolecular Energies from Experimental and Theoretical Structure Factors*. University at Buffalo, State University of New York, USA; University of Milan, Italy; University of Glasgow, UK; CNRISTM, Milan, Italy; and Middle Tennessee University, USA.
- Whitten, A. E., Turner, P., Klooster, W. T., Piltz, R. O. & Spackman, M. A. (2006). *J. Phys. Chem. A*, **110**, 8763–8776.